

Membrane microdomains from early gastrula embryos of medaka, *Oryzias latipes*, are a platform of E-cadherin- and carbohydrate-mediated cell–cell interactions during epiboly

Tomoko Adachi · Chihiro Sato · Yasunori Kishi · Kazuhide Totani · Takeomi Murata · Taichi Usui · Ken Kitajima

Received: 29 April 2008 / Revised: 14 August 2008 / Accepted: 18 August 2008 / Published online: 3 September 2008
© Springer Science + Business Media, LLC 2008

Abstract Formation of membrane microdomain is critical for cell migration (epiboly) during gastrulation of medaka fish [Adachi *et al.* (Biochem. Biophys. Res. Commun. 358:848–853, 2007)]. In this study, we characterized membrane microdomain from gastrula embryos to understand its roles in epiboly. A cell adhesion molecule (E-cadherin), its associated protein (β -catenin), transducer proteins (PLC γ , cSrc), and a cytoskeleton protein (β -actin) were enriched in the membrane microdomain. Le^X-containing glycolipids and glycoproteins (Le^X-gp) were exclusively enriched in the membrane microdomain. Interestingly, the isolated membrane microdomain had the ability to bind to each other in the presence of Ca²⁺. This membrane microdomain binding was achieved through the E-cadherin

homophilic and the Le^X-glycan-mediated interactions. E-cadherin and Le^X-gp were co-localized on the same membrane microdomain, suggesting that these two interactions are operative at the same time. Thus, the membrane microdomain functions as a platform of the E-cadherin- and Le^X-glycan-mediated cell adhesion and signal transduction.

Keywords Membrane microdomain · Lipid raft · Embryogenesis · Gastrulation · Epiboly · Cell adhesion · Medaka · Le^X · Cadherin · Glycopolymer · E-cadherin

Introduction

Membrane microdomains or lipid rafts are widely acknowledged as a hot spot for signal transduction [1], and co-localize glycosylphosphatidylinositol-anchored and membrane spanning receptor proteins with transducer proteins [2–5]. Membrane microdomains are isolated from various cells as a detergent-insoluble fraction having low buoyant density (the low density detergent-insoluble membrane, or LD-DIM) [6–10]. One of the interesting features of this domain is its enrichment in glycolipids in its outer surface [11], although not so often focused on. Several lines of evidence show that glycolipids in the membrane microdomain are involved in cell adhesion in early development [12], metastasis [13, 14], and signal transduction [7, 15]. Thus, the membrane microdomains may function in glycolipid-mediated cell adhesion, as well as in signal transduction. In our previous study, we first demonstrated the presence of membrane microdomains in gametic cells [10, 16] and have shown that the membrane

T. Adachi · C. Sato · Y. Kishi · K. Kitajima (✉)
Bioscience and Biotechnology Center, Nagoya University,
Nagoya 464-8601, Japan
e-mail: kitajima@agr.nagoya-u.ac.jp

T. Adachi · C. Sato · Y. Kishi · K. Kitajima
Graduate School of Bioagricultural Sciences,
Nagoya University,
Nagoya 464-8601, Japan

K. Totani · T. Murata · T. Usui
Department of Applied Biological Chemistry,
Faculty of Agriculture, Shizuoka University,
Ohyu 836,
Shizuoka 422-8529, Japan

Present address:

K. Totani
Department of Chemical Engineering,
Ichinoseki National College of Technology,
Ichinoseki City, Iwate 021-8511, Japan

microdomain of sperm acts as a binding site for sperm-binding protein of egg coat in an acidic glycolipids-dependent manner in sea urchin fertilization [17].

Recently we have also demonstrated that membrane microdomains or LD-DIM, occur in early gastrula embryos of medaka [18]. The embryonic LD-DIM is a cholesterol- and sphingomyelin-rich membrane. Cholesterol is a key lipidic component for the formation of LD-DIM, and its removal from biomembranes by methyl- β -cyclodextrin (MBCD) treatment disrupts the formation of LD-DIM [19]. Interestingly, when LD-DIM of early gastrula embryos is disrupted by MBCD treatment, the process of epiboly during gastrulation is impaired, leading to severe abnormality in normal developmental processes [18]. The 3 mM MBCD-induced disruption of the LD-DIM proceeds rapidly within 5 min¹. The disruption of LD-DIM and the subsequent impairment of gastrulation processes are also observed on the short-term treatment of C2-ceramide [18], which destroys the liquid-ordered phase of biomembranes [20]. Thus, the formation of LD-DIM on the embryonic cells is crucial for normal development of embryos. Furthermore, the MBCD-treated embryos that usually show severe abnormality during gastrulation returned to normal development when cholesterol is added back to the embryos 15 min after the MBCD treatment [18]. Thus, the disruption and restoration of the LD-DIM formation are reversible by the removal and addition of cholesterol, and eventually lead to abnormal and normal development, respectively. Notably, the most typical morphological feature on the LD-DIM disruption is a detachment of cells from the blastoderm and the enveloping layer, suggesting that the LD-DIM is involved in cell adhesion processes in the process of epiboly during gastrulation. These observations led us to a hypothesis that the membrane microdomains function as a platform of cell adhesion of blastodermal cells in epiboly during gastrulation. In the present study, to elucidate molecular mechanisms for the membrane microdomain-mediated cell adhesion, we characterized the LD-DIM in terms of its components and the homotypic adhesive nature.

Materials and methods

Medaka fish An orange-red variety of medaka (*Oryzias latipes*) was purchased from a local fish merchant (Sato Fish Farm, Yatomi, Japan) and bred in aquariums under a 14-h light/10-h dark cycle, at 27°C. Fertilized eggs were collected from the abdomens of females, and incubated in water at 27°C. Developmental stages of embryos were identified according to the criteria of Iwamatsu [21].

Materials A monoclonal mouse antibody against human CD15 or Lewis X (Le^X) (anti- Le^X) was purchased from Ancell Corp. (Bayport, MN, USA). A polyclonal rabbit anti-pan-cadherin antibody (anti-Cad) and a monoclonal mouse anti- β -actin were purchased from abcam (Cambridge, UK). A polyclonal rabbit anti- β -catenin was from Sigma (St. Louis, MO, USA). A monoclonal mouse antibody against the N-terminal extracellular domain (EC1) involved in the cadherin homophilic binding (anti-EC1) was prepared using a bacterially expressed recombinant EC1 as an immunogen.² A polyclonal rabbit anti-cSrc antibody and a monoclonal mouse anti-phospholipase C- γ (PLC γ) were purchased from Santa Cruz Biotechnology, Inc. (Santa Cruz, CA, USA). A horseradish peroxidase-conjugated goat antibody against mouse (IgG + IgM) was purchased from Zymed Laboratories (South San Francisco, CA, USA). A horseradish peroxidase-conjugated goat antibody against rabbit IgG was purchased from Cell Signaling Technology (Danvers, MA, USA). α -L-fucoside fucosylase (*Streptomyces* sp.142, α 1,3/1,4-specific fucosidase) was purchased from Takara (Kyoto, Japan). Pre-stained molecular weight marker was purchased from Bio-Rad (Hercules, CA, USA). LNFP-I (Fuc α 1 \rightarrow 2Gal β 1 \rightarrow 3GlcNAc β 1 \rightarrow 3Gal β 1 \rightarrow 4Glc), LNFP-II (Gal β 1 \rightarrow 3(Fuc α 1 \rightarrow 4) GlcNAc β 1 \rightarrow 3Gal β 1 \rightarrow 4Glc), LNFP-III (Gal β 1 \rightarrow 4 (Fuc α 1 \rightarrow 3)GlcNAc β 1 \rightarrow 3-Gal β 1 \rightarrow 4Glc) were purchased from Calbiochem (San Diego, CA, USA). LNFP I, LNFP II, and LNFP III were conjugated with phosphatidylethanolamine dipalmytoyl (PE) as described previously [22, 23], and designated H-Lac-PE, Le^a -Lac-PE, and Le^X -Lac-PE, respectively. Polyglutamic acid (PGA) conjugated with LacNAc (Gal β 1 \rightarrow 4GlcNAc) (LacNAc-PGA), Sia Le^X (NeuAc α 2 \rightarrow 3Gal β 1 \rightarrow 4(Fuc α 1 \rightarrow 3)GlcNAc β 1 \rightarrow 3Gal) (Sia Le^X -PGA), and Le^X (Gal β 1 \rightarrow 4(Fuc α 1 \rightarrow 3)GlcNAc β 1 \rightarrow 3Gal) (Le^X -PGA) were synthesized as described [24, 25].

Preparation of the LD-DIM or membrane microdomains LD-DIM fraction was prepared as described previously [10, 18]. In brief, embryos at early gastrula (12 h-post fertilization) of medaka (1.0 g) were homogenized in 5.0 ml of 10 mM sodium phosphate (pH 7.2), 0.15 M NaCl [phosphate-buffered saline (PBS)] containing 5 mM ethylene diamine tetraacetic acid (EDTA), 4 mU of leupeptin, and 12.6 mU of aprotinin. The homogenate was centrifuged at 4°C at 200,000 $\times g$ for 30 min to collect the membrane fraction as a pellet. The membrane fraction was suspended in 1.0 ml of 10 mM Tris-HCl (pH 7.5), 0.15 M NaCl, 5 mM EDTA (TNE) containing protease inhibitor cocktail and 1% Triton X-100, and stood on ice for 20 min. After

¹ Adachi, T., unpublished observation

² Adachi, T., Sato, C., Hashimoto, H., Wakamatsu, Y., and Kitajima, K., to be published elsewhere.

homogenized with ten strokes by Dounce homogenizer, the suspension was centrifuged at 4°C at 1,300×g for 5 min. The resultant supernatant was mixed with an equal volume of 85% (w/v) sucrose in TNE. The mixture was layered successively with 6 ml of 30% (w/v) sucrose in TNE and with 3.5 ml of 5% (w/v) sucrose in TNE, and centrifuged at 4°C at 200,000×g for 18 h. After centrifugation, 1 ml each of 11 fractions was collected from the top of the tube. Two peak fractions centered at fractions 3–5 (low density) and 10–11 (high density) were obtained. The fractions 3–5 contained a light scattering band, which corresponds to LD-DIM fraction (or membrane microdomain), while the fractions 10–11 contained Triton X-100 soluble materials, which is thus detergent-soluble membrane fraction (DSM). For chemical and immunochemical analyses, LD-DIM and DSM were dialyzed against water or PBS containing 5 mM EDTA. Unless otherwise stated, the amount of membrane fractions is expressed as protein quantity. Protein quantity was determined by the BCA assay kit (Pierce, Rockford, IL, USA) using bovine serum albumin (BSA) as a standard.

When the number of embryos was small, LD-DIM was prepared by the Opti-prep gradient method [26] with slight modification [18]. Briefly, homogenates of embryos were centrifuged at 4°C at 200,000×g for 30 min to collect the membrane fraction. The membrane fraction was suspended in 0.4 ml of 25 mM Tris-HCl (pH 7.0), 0.15 M NaCl, 5 mM EDTA containing the protease inhibitors (see above) and 1 % Triton X-100, and stood on ice for 20 min. The lysate was mixed with 0.8 ml of 60% (w/w) Optiprep (Sigma, St. Louis, MO, USA). The mixture was layered successively with 2 ml of 30% and with 0.5 ml of 5% Optiprep in the same buffer, and centrifuged at 4°C at 160,000×g for 4 h. After centrifugation, 0.5 ml each of eight fractions was collected from the top of the tube. Fractions 2–3 and 7–8 were pooled as LD-DIM and DSM fractions.

Enzyme-linked immunosorbent assay (ELISA) and thin-layer chromatography (TLC)-immunostaining of lipid fractions LD-DIM (41 µg) and DSM (350 µg) were lyophilized. To each lyophilized powder, 2 ml of chloroform/methanol (C/M; 2:1, v/v) were added and mixed. After centrifugation at 10,000×g for 15 min, the upper layer was set aside, and the lower layer was mixed with 2 ml of C/M (1:1, v/v), followed by centrifugation. The upper layer was set aside, and the lower layer received 2 ml of C/M/water (30:60:8, v/v/v), followed by centrifugation. The upper layer was combined with the two other upper layers described above and designated as total lipid fraction. The total lipid fraction was dried and dissolved with C/M/water (30:60:8, v/v/v). ELISA and TLC-immunostaining of the total lipid fraction were performed as previously described [27–29].

Western blotting Sodium dodecyl sulfate-polyacrylamide gel electrophoresis (SDS-PAGE) and electrotransfer to polyvinylidene difluoride (PVDF) membrane (Millipore, Bedford, MA, USA) and immunostained as described [30]. Briefly, the membrane was blocked with 1% BSA in PBS containing 0.05% Tween-20 (PBST) at room temperature for 1 h. After washing, the membrane was incubated with primary antibodies at 37°C for 2 h, or at 4°C for overnight for IgG antibodies, and at 4°C for overnight for IgM antibodies. The concentration of the primary antibodies was: 0.2 µg/ml for anti-Le^x; 1 µg/ml for anti-Cad; 8 µg/ml for anti-β-catenin; 0.4 µg/ml for anti-cSrc; 0.2 µg/ml for anti-PLCγ; 0.24 µg/ml for anti-β-actin. After washing twice with PBST, incubation of the membrane with secondary antibodies at 1:5,000 dilution with PBST containing 1% BSA were carried out at 37°C for 45 min. After washing three times in PBST, the membrane was developed using enhanced chemiluminescence reagent and HyperfilmTM MP (Amersham, Buckinghamshire, UK). Stained bands were quantitated densitometrically with ATTO Densitograph (Tokyo, Japan).

ELISA-based binding assay

1. *Coating efficiency of the well with LD-DIM:* 50 µl of 0–20 µg/ml LD-DIM purified from early gastrula embryos of 12 h-post fertilization were put into a well of 96-well-plates and incubated at 37°C for 2 h or at room temperature for overnight. After washing three times with PBS, blocking was performed with 100 µl of PBS containing 1% BSA at room temperature for 2 h. After washing three times with PBS, the well was incubated with 50 µl of anti-Le^x (2.0 µg/ml) at 4°C for overnight. After washing three times with PBST, incubation was performed with peroxidase-conjugated anti-mouse (IgG + IgM) antibody (1:500 dilution) in containing 1% BSA at 37°C for 45 min. After washing five times with PBST, the color development was performed in 100 µl of 0.05% *o*-phenylenediamine, 0.1 M Tris-HCl (pH 7.5) and 0.006% H₂O₂. After color development was stopped with 100 µl of 1 M sulfuric acid, absorbance at 490 nm was measured.
2. *LD-DIM homotypic binding:* Binding of biotinylated LD-DIM to LD-DIM was measured based on ELISA. To prepare biotinylated LD-DIM, 150 µg of purified LD-DIM was incubated with 4 µg of sulfo-NHS-biotin (Pierce) in 3 ml of 50 mM sodium bicarbonate at 4°C for 2 h. The biotinylated LD-DIM was dialyzed against 1 mM EDTA and PBS, and, if necessary, adjusted to 2 mM CaCl₂. Fifty microliters of 0–20 µg/ml (0–1.0 µg/well) LD-DIM purified from early gastrula embryos of 12 h-post fertilization were put into a well of 96-well-plates and incubated at 37°C for 2 h or at room temperature for overnight. After washing three

times with PBS, blocking was performed with 100 μ l of 1%BSA/PBS at room temperature for 2 h. After washing three times with PBS, 50 μ l of 20 μ g/ml biotinylated LD-DIM was added and incubated at room temperature for 2 h or at 4°C for overnight. After washing with PBS, the well was incubated with 50 μ l of avidin-biotin peroxidase complex solution (Vector Laboratory, Burlingame, CA, USA) at room temperature for 30 min. After washing five times with PBS, the bound biotinylated LD-DIM was quantified by color development as described above.

3. *LD-DIM binding to synthetic glycoconjugates:* For binding of the biotinylated LD-DIM to neoglycopolypeptides (LacNAc-PGA, SiaLe^X-PGA, and Le^X-PGA; see Fig. 6A), the wells were coated with 50 μ l of 0–8 μ g/ml neoglycopolypeptides in PBS, and blocked. For binding to neoglycolipids (H-Lac-PE, Le^a-Lac-PE, Le^X-Lac-PE, and PE; see Fig. 6D), the wells were coated with 50 μ l of 0–20 μ g/ml of the neoglycolipids in ethanol, dried at 37°C, and blocked.
4. *Effect of protease treatment:* For protease treatment, the LD-DIM coated on the well was treated with 100 μ l of 400 ng/ml of Actinase E (Waken, Japan) in PBS at room temperature for 12 h. After washing with PBS, the wells were blocked, followed by the binding assay as described above.
5. *Effect of periodate oxidation:* For periodate oxidation of neoglycopolypeptides or LD-DIM, each neoglycopolypeptide or the LD-DIM coated on the well was treated with 100 μ l of 2.5 mM NaIO₄ in 40 mM sodium acetate buffer (pH 5.5) at 4°C for 3 h in the dark. After washing three times with water, 100 μ l of 0.1 M sodium borohydride in 0.1 M sodium borate buffer (pH 8.0) was added to the wells and incubated at room temperature for 3 h. After washing with PBS, the binding assay followed.
6. *Effect of fucosidase treatment:* For fucosidase treatment of LD-DIM, the LD-DIM coated on the well was treated with 100 μ l of 5 mU/ml of α -L-fucosidase (*Streptomyces* sp.142, α 1,3/1,4-fucosidase) in 10 mM sodium phosphate buffer (pH 6.0) and incubated at room temperature for 12 h. After washing with PBS, the binding assay followed.
7. *Effect of combined treatments with protease and periodate oxidation, or fucosidase:* The LD-DIM coated on the well was subjected to Actinase E digestion followed by periodate oxidation, and to fucosidase digestion followed by Actinase E digestion. Between the treatments, the well was washed well with PBS. The binding assay followed.
8. *Effect of the inhibition peptide for the homophilic binding of E-cadherin:* The wells were coated with 50 μ l of 10 μ g/ml LD-DIM, and incubated with 50 μ l

of 0–10 μ M of the peptides in PBS. After washing and blocking with 1%BSA-PBS for 1 h, the biotinylated LD-DIM (10 μ g/ml) was added and incubated in the presence of 2 mM CaCl₂ in 50 μ l PBS at room temperature for 2 h. Other procedures were performed as described above. An inhibition peptide for homophilic binding of cadherin, HAD (LLAHADVED), was designed based on the amino acid sequence of medaka E-cadherin.³ Two unrelated peptides with cadherin family, Pep1 (DGSGADTVH) and Pep2 (DDAT-SEAATGPSG), were also used for the inhibition experiment. These synthetic peptides were provided by TANA Laboratories, L. C. (Houston, TX, USA).

Immunoprecipitation experiments before and after LD-DIM disruption with MBCD treatment Anti-EC1 (10 μ g) was mixed with 40 μ l of protein G-Sepharose/PBS (1:1, v/v) at 4°C for 1 h with a rotator. After centrifugation at 200 \times g for 1 min, the precipitate was washed three times with PBS to obtain anti-EC1-Sepharose. Membrane fractions were prepared from early gastrula embryos (see above) in the presence or absence of 10 mM MBCD in PBS for 30 min at 27°C, and mixed with the anti-EC1-Sepharose at 4°C for overnight with a rotator. After centrifugation at 200 \times g for 1 min, the precipitate was subjected to SDS-PAGE-Western blotting using anti-Cad (1:500 dilution) or anti-Le^X as described [30].

Results

LD-DIM of early gastrula embryos contains not only cell adhesion molecules and transducer proteins but also Le^X-containing glycoproteins and glycolipids We have recently demonstrated that LD-DIM prepared from medaka early gastrula embryos is enriched in cholesterol and sphingomyelin and contains a high-molecular weight (>350,000) glycoprotein containing Le^X structure, Le^X-gp [18]. In the present study, we examined if the LD-DIM also contained the Le^X-containing glycolipids. The LD-DIM and DSM fractions were prepared by sucrose density gradient centrifugation of the Triton X-100-treated membrane fraction of early gastrula embryos. Eleven 1-ml fractions were collected from the top of the centrifugation tube, and two fractions centered at fractions 3–5 (low density, light scattering) and 10–11 (high density) were collected as LD-DIM and DSM, respectively. The lipid fractions were then prepared from the LD-DIM and DSM. The major lipid compositions for LD-DIM and DSM were reported and

³ Adachi, T., Sato, C., Hashimoto, H., Wakamatsu, Y., and Kitajima, K., to be published elsewhere.

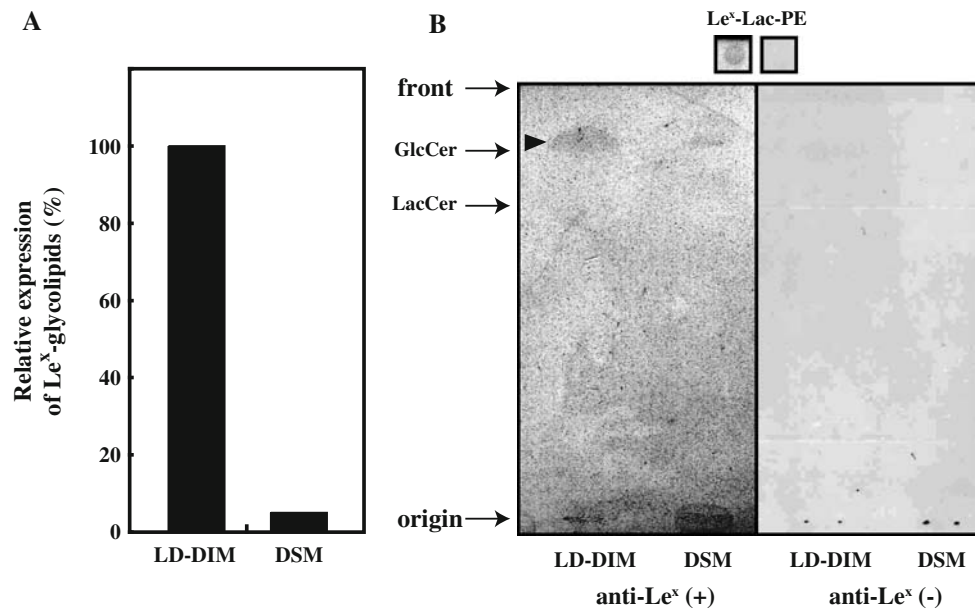


Fig. 1 Identification of Le^X-containing glycolipids in LD-DIM from medaka gastrula embryos. **A** ELISA analysis of neutral lipids prepared from the LD-DIM (membrane microdomain) and DSM. The wells were coated with the LD-DIM- or DSM-derived neutral lipid fractions, blocked with 1% BSA/PBS at room temperature for 2 h, and incubated with anti-Le^X (2 μg/ml), followed by incubating with a horseradish peroxidase-conjugated goat antibody against mouse (IgG + IgM) (1:1,000 dilution) as a secondary antibody. Color development was then performed with 0.05% *o*-phenylenediamine, 0.1 M Tris-HCl (pH 7.5) and 0.006% H₂O₂, and the absorbance at 490 nm was measured. All the experiments were carried out at least in duplicate and the deviations are within the symbols. **B** TLC-immunostaining of the neutral lipid fractions from the LD-DIM and DSM. After development of the samples in a solvent C/M/0.25% CaCl₂ (55:45:10, v/v/v), the

TLC plate was coated with polyisobutylmethacrylate (Sigma, St. Louis, MO, USA), blocked with PBS containing 1% BSA and 1% polyvinylpyrrolidone, and incubated with anti-Le^X (2 μg/ml) as a primary antibody, followed by incubating with a horseradish peroxidase-conjugated goat antibody against mouse (IgG + IgM; 1:500 dilution) as a secondary antibody. Color development was then performed with diaminobenzidine. Le^X-Lac-PE (20 ng) was spotted as a positive control on the same TLC plate after development of the samples and subjected to the immunostaining (upper panels). anti-Le^X (+), with primary antibody; anti-Le^X (-), without primary antibody. Le^X-glycolipid is detected (arrowhead). The migration positions for glucosyl ceramide (GlcCer) and lactosyl ceramide (LacCer) are indicated by the arrows

neutral glycolipids are more than ten-fold abundant than acidic glycolipids [18]. The lipid fractions were analyzed for the presence of Le^X structure by ELISA using anti-Le^X. The Le^X structure was detected in neutral lipid fractions from LD-DIM, but not DSM (Fig. 1A). The anti-Le^X did not bind Le^X-related structures such as LacNAc (Galβ1–4GlcNAc), sialyl-Le^X (Neu5Acα2–3Galβ1–4(Fucα1–3)GlcNAc), or Gal-Le^X (Galβ1–4Galβ1–4(Fucα1–3)GlcNAc) (data not shown). The Gal-Le^X is an abundant epitope of major cortical vesicular glycoproteins in medaka eggs [31]. The mAb.3D11 specifically recognizing Gal-Le^X did not bind Le^X-structures (data not shown). Therefore, the anti-Le^X is highly specific to Le^X structure. An Le^X-containing glycolipid, Le^X-glycolipid, was detected by TLC immunostaining of the lipid fraction of LD-DIM, while also detected in that of DSM at a low level, a 19th of that in LD-DIM (Fig. 1B). These results indicate the Le^X-glycolipid is enriched in LD-DIM.

It has been shown that cell adhesion molecules and transducer proteins are localized in LD-DIM or rafts [32–34]. In early development of *Xenopus*, a cell adhesion

molecule, cadherin, and transducer proteins, cSrc and PLCγ, play important roles [35, 36], although whether these proteins occur in medaka embryos has remained unknown. We thus examined whether these proteins are present in the LD-DIM isolated from medaka embryos at early gastrula stage by Western blotting (Fig. 2). E-cadherin was exclusively detected as three components from 128 to 104 kDa in LD-DIM, but not in DSM, using anti-EC1, which recognizes the extracellular medaka E-cadherin repeat domain 1⁴. β-Catenin, which binds to the intracellular domain of various cadherin molecules to regulate their functions [37], was detected at 93 kDa in LD-DIM, although very little in DSM. In addition, cSrc, a member of Src tyrosine kinase family, was detected at 60 kDa in LD-DIM, but not in DSM, consistent with the fact that cSrc tends to be recruited to LD-DIM due to its modification by saturated fatty acids such as palmitic and myristic acids [32]. An exclusive localization of PLCγ in LD-DIM was

⁴ Adachi, T., Sato, C., Hashimoto, H., Wakamatsu, Y., and Kitajima, K., to be published elsewhere.

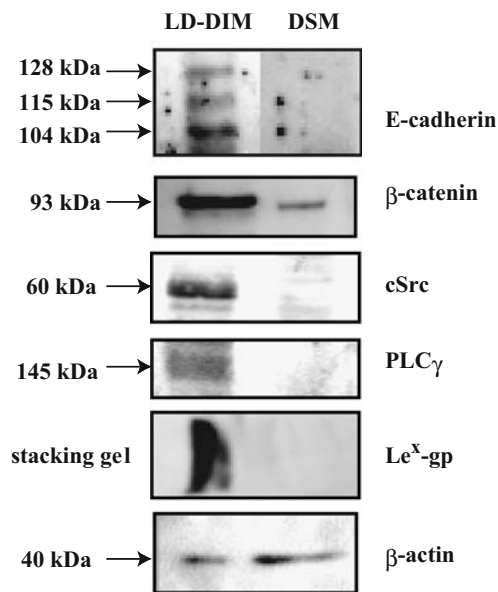


Fig. 2 Western blotting of the LD-DIM and DSM from early gastrula embryos. The LD-DIM and DSM (10 μg as proteins/lane) were subjected to SDS-PAGE (10% PAG) and transferred to PVDF membrane. Protein components were detected by immunostaining using antibodies that specifically recognizes those proteins indicated at the right side of each panel. The number with the arrow indicates the molecular size (*Mr*). For E-cadherin, the immunoprecipitate of LD-DIM or DSM (60 μg each) with anti-EC1, an antibody against the extracellular domain involved in cadherin–cadherin homophilic binding, was subjected to Western blotting using anti-Cad. E-cadherin gave three components that are different in *N*-linked glycan structures (data not shown). Primary antibodies used are; anti-Cad (1 $\mu\text{g}/\text{ml}$), anti- β -catenin (8 $\mu\text{g}/\text{ml}$), anti-cSrc (0.4 $\mu\text{g}/\text{m}$), anti-PLC γ (0.2 $\mu\text{g}/\text{ml}$), anti-Le^X (0.2 $\mu\text{g}/\text{ml}$), and anti-actin (0.24 $\mu\text{g}/\text{ml}$)

also observed at 145 kDa. Furthermore, the Le^X-containing glycoprotein (Le^X-gp) was exclusively detected at stacking gel in LD-DIM, but not in DSM, as described previously [18]. It should be noted that β -actin was detected at 40 kDa in both LD-DIM and DSM as reported previously [38, 39]. These results indicate that the cell adhesion molecule (cadherin), its associated protein (β -catenin), transducer

proteins (cSrc, PLC γ), and Le^X-gp, except β -actin, are enriched in medaka embryonic LD-DIM.

Le^X-gp expression increases during gastrulation while the LD-DIM is constantly formed To understand developmental changes of the amount of LD-DIM, the LD-DIM fractions isolated from embryos at 0, 6, 12, 18, 24, and 30 h after fertilization were analyzed for the protein amount (Table 1). The proportion of the protein amount of LD-DIM to that of the whole membrane fraction was largely constant at 17–21% during early development, while the yields of protein amount in whole membrane fractions were deviated from samples to samples probably due to experimental errors. Cholesterol was also quantified, because it is a key component for LD-DIM formation [18]. The proportion of the amount of cholesterol in LD-DIM to that in the whole membrane fraction was also constant at 12–14% (Table 1). These results indicate that LD-DIM is constantly formed in developing embryos and that the protein and cholesterol amounts in LD-DIM remains unchanged at least during gastrulation [6, 12, and 18 h post-fertilization (hpf)].

Le^X-gp is exclusively localized in LD-DIM at early gastrula embryo (12 hpf) [18]. The developmental change of Le^X-gp was examined by Western blotting of fractions obtained by the Opti-prep method from whole membrane fractions (Fig. 3A). The expression of Le^X-gp was first detected at 12 hpf and increased at least until late gastrula stage (30 hpf). Le^X-gp was exclusively detected at the stacking gel at any stages examined (Fig. 3A), and mostly at the LD-DIM fraction (lanes 2, 3) rather than at the DSM fraction (lanes 7, 8). However, at later stages (24–30 hpf), membrane fractions with higher densities than LD-DIM (lanes 4–6) increased. Developmental expression of Le^X-gp in embryos was summarized in Fig. 3B. The expression of Le^X-gp increased at gastrulation stages when epiboly was going on. Considering that the amount of LD-DIM remains unchanged, these results indicate that the density of Le^X-gp in LD-DIM increases during epiboly. However, whether the

Table 1 Protein and cholesterol amounts in LD-DIM during early development

| Stage (hpf) | Protein | | | Cholesterol | | |
|-------------|--|---------------------------------------|------------------|--|---------------------------------------|------------------|
| | LD-DIM ($\mu\text{g}/\text{embryo}$) | Whole ($\mu\text{g}/\text{embryo}$) | LD-DIM/whole (%) | LD-DIM ($\mu\text{g}/\text{embryo}$) | Whole ($\mu\text{g}/\text{embryo}$) | LD-DIM/whole (%) |
| 0 | 0.26 | 1.5 | 17 | n.d. | n.d. | n.d. |
| 6 | 0.26 | 1.2 | 21 | 0.041 | 0.31 | 14 |
| 12 | 0.093 | 0.46 | 21 | 0.032 | 0.27 | 12 |
| 18 | 0.43 | 2.5 | 17 | 0.029 | 0.21 | 14 |
| 24 | 0.37 | 1.9 | 19 | n.d. | n.d. | n.d. |
| 30 | 0.21 | 1.1 | 20 | n.d. | n.d. | n.d. |

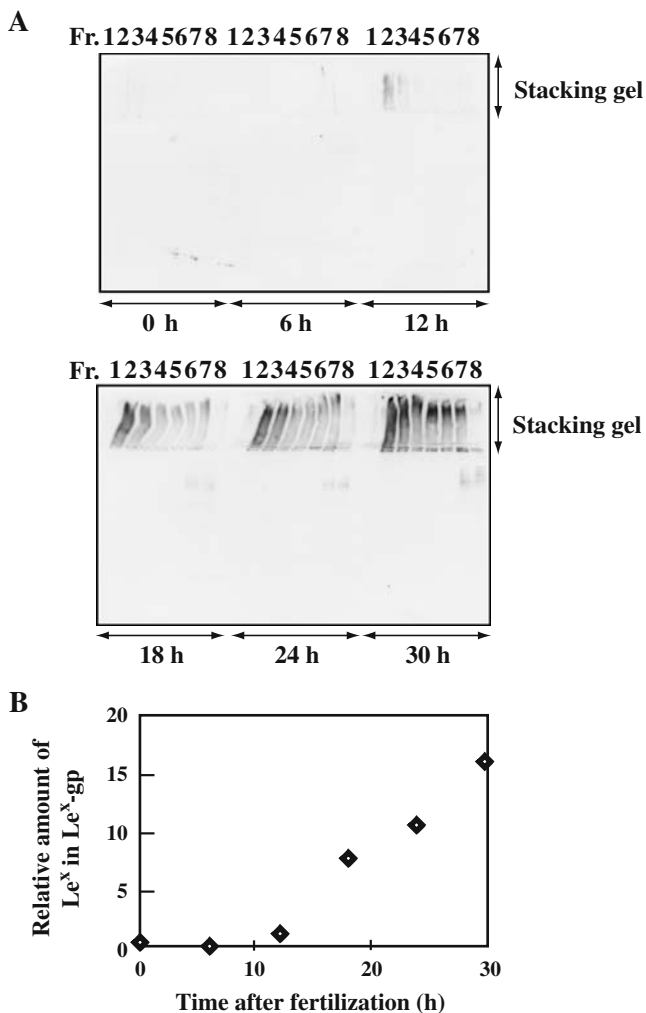


Fig. 3 Developmental changes in the amount of Le^X-gp in the membrane fraction from embryos after fertilization until late gastrula stage. **A** Embryos were collected at 0 h (just fertilized), 6 h (late morula), 12 h (early gastrula), 18 h (mid gastrula), 24 h (late gastrula), and 30 h (2–4 somite stage) after fertilization. The whole membrane fraction prepared from a hundred embryos of each stage was subjected to the LD-DIM preparation by the Optiprep method, and eight fractions separated from the top to bottom of the centrifugation tube (Fr. 1–8) were analyzed by SDS-PAGE (3.5% PAG for stacking gel; 10% PAG for separating gel) followed by immunoblotting using anti-Le^X as described under “Materials and methods”. Fractions 2–3 and 7–8 are the LD-DIM and DSM, respectively. **B** The relative amount of the Le^X-gp in embryos of each developmental stage. Intensity of the immunostaining of the stacking gel region of each lane was densitometrically quantified on ATTO Densitograph, and those intensity values were summed under each stage. The values represent the relative amount of Le^X-gp to that for embryos of 12 h post-fertilization set as 1.0

Le^X-gp in higher density fractions at later stages is the same as the Le^X-gp in the LD-DIM remains unknown until the carrier proteins of Le^X-glycans are identified. Identification of Le^X-gp and elucidation of the glycosylation profiles on the Le^X-gp are important future subjects.

LD-DIM homotypically binds to LD-DIM in a protein- and a glycan-dependent manners Le^X structure is known to have the ability to bind each other, which mediates cell–cell adhesion, *i.e.*, compaction, in mouse embryos at morula stage [40, 41]. Because Le^X-gp and Le^X-glycolipid is highly expressed on the LD-DIM in epiboly process in medaka embryo, LD-DIM is suggested to be involved in cell–cell interaction in epiboly. In addition, E-cadherin, which is also involved in compaction through cadherin–cadherin homophilic binding [42, 43], is also localized in LD-DIM. Therefore, it is suggested that the LD-DIM is a membrane microdomain involved in cell adhesion between embryonic cells. To demonstrate if LD-DIM exhibits adhesive nature to each other, the ELISA-based binding assay was performed using the LD-DIM isolated from early gastrula embryos (Fig. 4). The coating efficiency of the LD-DIM was first examined (Fig. 4A). The LD-DIM coated on the well was increased depending on increasing amounts of added LD-DIM, and saturated at 0.5–1.0 μg/well. Then, biotinylated LD-DIM (1 μg/well) was added to the LD-DIM-coated wells at 0–1 μg/well (Fig. 4B). The biotinylated LD-DIM bound the LD-DIM on the well in a dose-dependent manner in the presence of 1 mM Ca²⁺. On the other hand, no binding was observed in the absence of Ca²⁺. These results show that early gastrula embryonic LD-DIM has the ability to bind homotypically in the presence of Ca²⁺. It should be noted that the LD-DIM homotypic binding shows exponential, but not saturation curve in the presence of Ca²⁺. This may be due to homotypic interaction of the LD-DIM with polyvalent binding sites, which may leads to unsaturated aggregation of biotinylated LD-DIM accumulated on the LD-DIM on the well. In this regard, it was previously reported that BSA conjugated with several sulfated disaccharide units involved in sponge cell adhesion forms the polyvalent multilayer on the monolayer surface of the sulfated disaccharide-conjugated BSA in the presence of 10 mM Ca²⁺ [44].

To examine which components of the LD-DIM were involved in the LD-DIM homotypic binding, LD-DIM-coated wells were subjected to protease treatment, periodate oxidation or fucosidase treatment (Fig. 4C,D). The LD-DIM homotypic binding was decreased when the coated LD-DIM was treated with Actinase E protease (Fig. 4C). The binding was 54% of that without protease treatment. No further decrease was observed even when the dose of the protease was increased (data not shown). These results suggest that the LD-DIM homotypic binding was mediated at least in part by proteins like E-cadherin. On the periodate oxidation treatment of the coated LD-DIM, the LD-DIM homotypic binding was decreased to 53% of that without periodate oxidation (Fig. 4C). In addition, the treatment of the coated LD-DIM with α1,3/4-linkage specific fucosidase decreased the LD-DIM homotypic binding by 53%

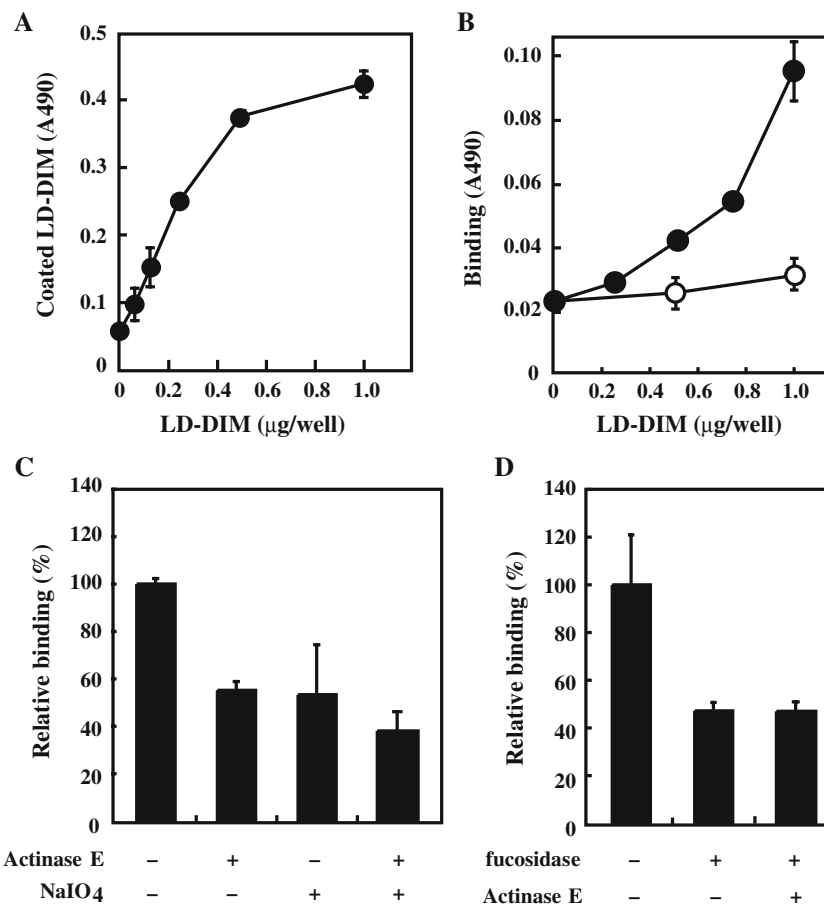


Fig. 4 LD-DIM-to-LD-DIM interaction of medaka gastrula embryo. **A** Coating efficiency of the well with LD-DIM. The well was coated with LD-DIM at 0–1.0 $\mu\text{g}/\text{well}$, and the coated LD-DIM was immunochemically quantitated. The experiments were performed in duplicate and the deviations are shown by the bars. **B** Binding of biotinylated LD-DIM to the coated LD-DIM. The well was coated with LD-DIM at 0–1.0 $\mu\text{g}/\text{well}$. After washing and blocking with 1% BSA/PBS, the biotinylated LD-DIM (1.0 $\mu\text{g}/\text{ml}$) was incubated in the presence (filled circle) or absence (unfilled circle) of the 2 mM Ca^{2+} at room temperature for 2 h. The bound LD-DIM was quantified as described under “Materials and methods”. All the experiments were performed at least in duplicate and the deviations are within 4%. **C**

Effects of Actinase E digestion followed by periodate oxidation. The well was coated with the LD-DIM at 1.0 $\mu\text{g}/\text{well}$, and treated with (+) or without (-) Actinase E. After washing, the well was treated with (+) or without (-) periodate (NaIO_4). After washing, the binding assay followed. **D** Effects of fucosidase digestion followed by Actinase digestion. The well was coated with the LD-DIM at 1.0 $\mu\text{g}/\text{well}$, and treated with (+) or without (-) α -L-fucosidase. After washing, the well was treated with (+) or without (-) Actinase E. After washing, the binding assay followed. All the experiments for C, and D were performed at least in duplicate and the deviations are shown by the bars

(Fig. 4D). These results indicate that glycan chains are involved in the LD-DIM homotypic binding, and that Fuc-containing glycans like Le^x structure are important. Taken all together, the protein-mediated and glycan-mediated interactions are involved in the LD-DIM homotypic binding. To gain a further insight into the mechanism of the LD-DIM homotypic binding, the effect of combined disruption of protein and glycan components of the coated LD-DIM on the biotinylated LD-DIM binding was examined. The protease digestion followed by the periodate oxidation decreased the binding to 37% of that without any treatments (Fig. 4C). Similarly, the fucosidase treatment followed by the protease digestion also decreased the binding to 47% of that without any treatments (Fig. 4D).

Thus, the combined treatments did not result in a complete loss of the binding, suggesting that unknown interactions, such as lipid-mediated one, other than the glycan- or protein-mediated interaction may contribute to the LD-DIM homotypic interaction in the presence of Ca^{2+} . In addition, contributions of the protein- and the glycan-mediated interactions to the LD-DIM homotypic binding were not additive. Both protein- and glycan-mediated interactions may mutually affect each other on the same LD-DIM. However, to understand underlying mechanisms for the LD-DIM homotypic interaction precisely, many questions will have to be solved: What are the unknown interactions like? How is the surface organization of the proteins and glycans involved in the binding? What are specific

functions of the common glycan structures on glycolipids and glycoproteins?

LD-DIM homotypic binding is mediated by E-cadherin Because E-cadherin occurs in the embryonic LD-DIM (Fig. 2), an E-cadherin–E-cadherin homophilic binding is suggested to mediate the LD-DIM–LD-DIM homotypic binding. The decapeptide sequence in the extracellular domain 1 that is involved in the cadherin-cadherin homophilic binding inhibits the cadherin-mediated binding [45]. To demonstrate the involvement of cadherin in the LD-DIM homotypic binding, we performed the inhibition experiment using an inhibitory peptide for the E-cadherin homophilic binding (HAD, LLAHADVED), which is designed from the amino acid sequence of medaka E-cadherin⁵. HAD inhibited the LD-DIM homotypic binding in a dose-dependent manner (Fig. 5). The binding was inhibited by 60% by 10 μ M HAD, while the cadherin-unrelated peptides, Pep1 and Pep2, had no effect on the binding at up to 10 μ M. These results indicate that E-cadherin is involved in the LD-DIM homotypic binding. Considering that 30% inhibition of the binding was already attained by 1 μ M HAD, inhibition by 10 μ M HAD appears to be saturated. This may suggest that some interactions, such as a glycan-mediated one, other than E-cadherin-mediated interaction are operated in the LD-DIM homotypic binding.

LD-DIM binds to Le^X-structures We then asked whether the Le^X-structure are involved in the LD-DIM homotypic binding. We performed an ELISA-based binding assay using various solidified synthetic glycoconjugates as a binding counterpart for the biotinylated LD-DIM. The biotinylated LD-DIM was shown to bind to a synthetic glycopolypeptide Le^X-PGA (Fig. 6A,B), and this binding was completely abrogated when Le^X-PGA was treated with periodate oxidation (Fig. 6C). Thus, a glycan part of Le^X-PGA, but not the polypeptide PGA, is involved in the LD-DIM binding. Binding to LacNAc-PGA was 20% of that to Le^X-PGA (Fig. 6B). Consistent with this result, α 1,3/4-linkage specific fucosidase treatment of Le^X-PGA on the well greatly decreased the LD-DIM binding (data not shown). No binding to SiaLe^X-PGA was detected (Fig. 6B). Thus, the removal of Fuc residue from or the addition of Sia residue to Le^X-PGA negatively affected the LD-DIM binding. These results indicate that the trisaccharide structure of Le^X is involved in the binding.

We further examined the structural requirement for the LD-DIM binding using phosphatidylethanolamine-conjugated glycans, H-Lac-PE, Le^a-Lac-PE, and Le^X-Lac-PE, as

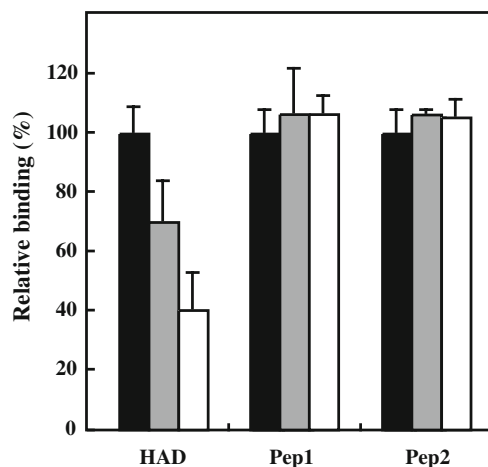


Fig. 5 Effect of the inhibition peptide for the E-cadherin homophilic binding on the LD-DIM-to-LD-DIM interaction. The wells were coated with LD-DIM at 0.5 μ g/well, and incubated with 0 μ M (black), 1 μ M (gray), and 10 μ M (white) of the peptides in PBS at room temperature for 1 h, followed by the binding assay. HAD (LLAHADVED), an inhibition peptide for homophilic binding of E-cadherin; Pep1 (DGSADTVH) and Pep2 (DDATSEATGPSG), unrelated peptides with E-cadherin. All the experiments were performed in duplicate and the deviations are shown by the bars

a binding counterpart for the biotinylated LD-DIM (Fig. 6D,E). The biotinylated LD-DIM dose-dependently bound to Le^X-Lac-PE, H-Lac-PE, and Le^a-Lac-PE, but not to PE. The binding to Le^X-Lac-PE was twice as high as that to H-Lac-PE or Le^a-Lac-PE. These results suggest that at least the presence of Fuc residues is important for the glycan-mediated binding of LD-DIM. Since either H- or Le^a-structure was not detected in LD-DIM (data not shown), Le^X-structure may be responsible for the binding.

E-cadherin and Le^X-gp are colocalized in the identical LD-DIM, but not tightly associated with each other The LD-DIM homotypic binding is mediated by E-cadherin and Le^X-structures as described above. We then ask whether E-cadherin and Le^X-structures are localized in the identical or different LD-DIM. To answer this question, immunoprecipitation experiments in the presence or absence of MBCD were performed using anti-EC1, which recognizes the extracellular domain of medaka E-cadherin involved in the homophilic binding. We previously showed that the LD-DIM was disrupted in the presence of MBCD [18]. The Le^X-gp and E-cadherin were both detected in the immunoprecipitate with anti-EC1 in the absence of MBCD (Fig. 7). On the other hand, Le^X-gp was not detected in the anti-EC1-derived immunoprecipitate from the LD-DIM fraction prepared in the presence of MBCD, while E-cadherin was detected. These results indicate that E-cadherin and Le^X-gp are tethered on the identical LD-DIM, but that they do not form physically stable complex on the membrane. These results also suggest that E-cadherin- and

⁵ Adachi, T., Sato, C., Hashimoto, H., Wakamatsu, Y., and Kitajima, K., to be published elsewhere.

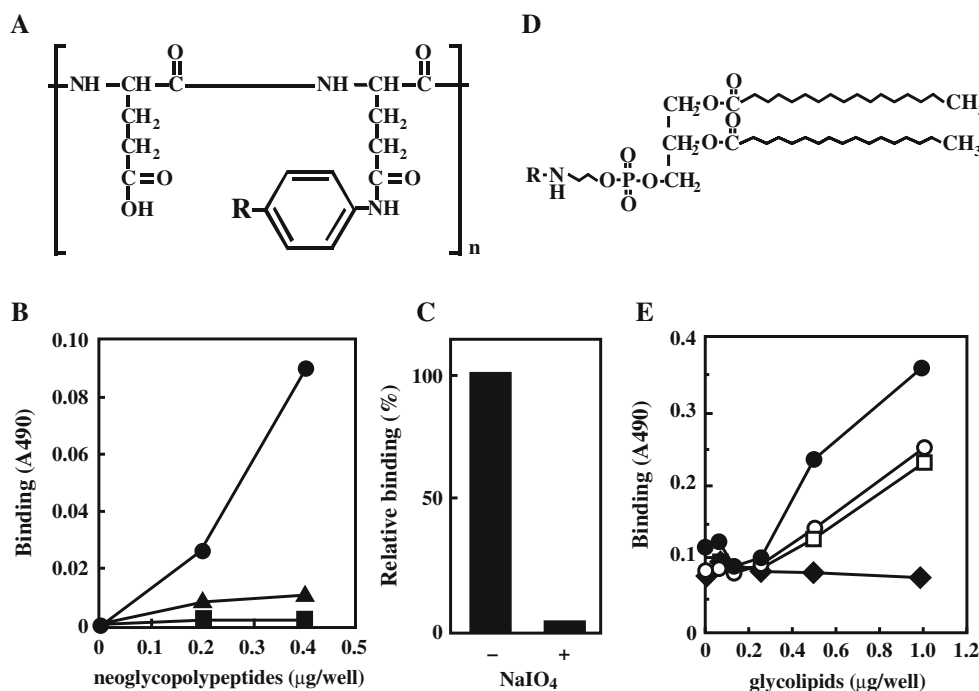


Fig. 6 Binding of LD-DIM from medaka gastrula embryos to the Le^X-containing neoglycoconjugates. **A** Structure for neoglycopolypeptides. Le^X-PGA, R=Galβ1–4 (Fucα1–3)GlcNAcβ1–; LacNac-PGA, R=Galβ1–4GlcNAcβ1; SiaLe^X-PGA, R=Siaα2–3Galβ1–4(Fucα1–3)GlcNAcβ1. *n*=363. **B** Binding of LD-DIM to neoglycopolypeptides. The wells were coated with Le^X-PGA (closed circle), LacNac-PGA (closed triangle), or SiaLe^X-PGA (closed square) at 0–0.4 µg/well. After washing and blocking with 1% BSA in PBS, the wells were incubated with the biotinylated LD-DIM (10 µg/ml) in the presence of the 2 mM Ca²⁺ at room temperature for 2 h. The bound LD-DIM was quantitated. **C** Effect of periodate oxidation on the LD-DIM binding to Le^X-PGA. The

wells coated with Le^X-PGA at 1.0 µg/well were treated with (+) or without (–) periodate oxidation, followed by the binding experiment as described in **B**. **D** Structure for neoglycolipids. H-Lac-PE, R=Fucα1–2Galβ1–3GlcNAcβ1–3Galβ1–4Glc'; Le^a-Lac-PE, R=Galβ1–3 (Fucα1–4)GlcNAcβ1–3Galβ1–4Glc'; Le^X-Lac-PE, R=Galβ1–4(Fucα1–3)GlcNAcβ1–3Galβ1–4Glc'; PE, R=H. **E** The wells were coated with H-Lac-PE (open square), Le^a-Lac-PE (open circle), Le^X-Lac-PE (closed circle), or PE (closed diamond) at 0–1.0 µg/well. After washing and blocking with 1% BSA in PBS, the binding experiment was performed as described in **B**. All the experiments for **B**, **C**, and **E** were carried out at least in duplicate and the deviations are within 4%

Le^X-mediated interactions can be operative at the same time. Interestingly, E-cadherin contains no Le^X-structure on the molecule.

Discussion

We recently demonstrated that formation of membrane microdomain or LD-DIM of gastrula embryos is crucial for cell adhesion in the progress of epiboly during gastrulation [18]. In the present study, we sought to elucidate how the membrane microdomain is involved in the cell adhesion process. We first characterized components of the LD-DIM, and showed the presence of a cell adhesion molecule (E-cadherin), its associated protein (β-catenin), transducer proteins (cSrc, PLCγ) and a cytoskeleton protein (β-actin) in the membrane microdomains or LD-DIMs of medaka gastrula embryo, consistent with the known common properties of membrane microdomains [32–34]. We previously showed that gastrula embryo LD-DIM is the cholesterol-

ol- and sphingomyelin-enriched membrane, and that a large glycoprotein containing Le^X-structure (Le^X-gp) is unique to and enriched in the medaka embryonic LD-DIM [18]. In the present study, we showed that the gastrula embryo LD-DIM also contains a Le^X-glycolipid. Taken all together, we propose a hypothetical model of membrane microdomains or LD-DIMs of medaka gastrula embryos (Fig. 8).

E-cadherin is an essential protein involved in cell adhesion through its homotypic binding in embryogenesis and development [42, 43, 46]. In medaka embryos, E-cadherin and β-catenin are exclusively localized in the membrane microdomain and co-localized with β-actin (Fig. 2). β-catenin binds to the intracellular domain of cadherin molecules on one side, and to actin filament through α-catenin on the other side [37, 47, 48]. Thus, an adhesion complex consisting of E-cadherin, α- and β-catenin, and β-actin must form in the membrane microdomain of medaka gastrula embryos. Proliferation and migration of blastodermal cells occurs during epiboly [49]. cSrc and PLCγ are implicated in cell proliferation process during early development [35, 36]. It is reported that these

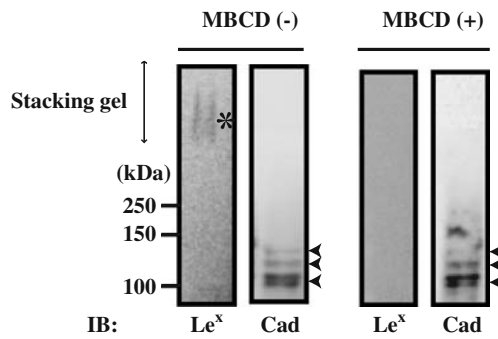


Fig. 7 Co-localization of E-cadherin with Le^X -gp in the LD-DIM as revealed by the immunoprecipitation experiment. Membrane fraction prepared from early gastrula embryos were immunoprecipitated with anti-EC1 recognizing the extracellular domain involved in the E-cadherin homophilic binding in the presence (+) or absence (-) of 10 mM MBCD. The precipitates were analyzed by Western blotting (7.5% PAG) using anti- Le^X (IB: Le^X) or anti-Cad (IB: Cad) as a primary antibody. The *arrowheads* and the *asterisk* indicate E-cadherin molecules and Le^X -gp, respectively. Molecular sizes (*Mt*) for marker proteins are shown on the *left side of the panel*

proteins are membrane microdomain-resident components, consistent with our observation. Co-localization of E-cadherin with cSrc kinase on membrane microdomains has not directly demonstrated, but it has been long known that cadherin and cSrc family kinases are localized in the cell–cell adherens junctions [50]. A recent report shows that E-cadherin-mediated cell adhesion activates cSrc signaling in CHO cells [51]. Although whether cadherin and the cSrc physically contact with each other is not known, these proteins may be co-localized in the membrane microdomain. cSrc is modified by palmitoylation and myristoylation to be recruited to the membrane microdomain [32]. Co-localization of E-cadherin and PLC γ has not been reported either. In pheochromocytoma PC12 cell, PLC γ is recruited to the membrane microdomain when EGF receptor is activated, although usually a cytosolic protein [34]. Once EGF binds to its receptor, activation of a Src kinase by phosphorylation and the subsequent Src-dependent phosphorylation of EGF receptor occur, followed by the recruit of PLC γ into the membrane microdomain. Thus, the activation of receptor and the downstream signal transduction occur on the membrane microdomain. In gastrulation of African claw frog embryo, PLC γ associates with an phosphorylated FGF receptor (activated form) [35].

In the present study, we also demonstrated that the membrane microdomains or LD-DIMs from gastrula embryos show the homotypic binding in the presence of Ca^{2+} (Fig. 4). Ca^{2+} is essential for this homotypic binding, because no binding happens in the absence of Ca^{2+} . Two molecular mechanisms for the homotypic LD-DIM binding are involved: One is a protein–protein interaction that is mediated through a homophilic binding of E-cadherin on the

membrane microdomain, and the other is a carbohydrate-mediated interaction in which the Le^X -glycans are involved.

The involvement of E-cadherin in the LD-DIM homotypic binding was shown by the inhibition experiment using

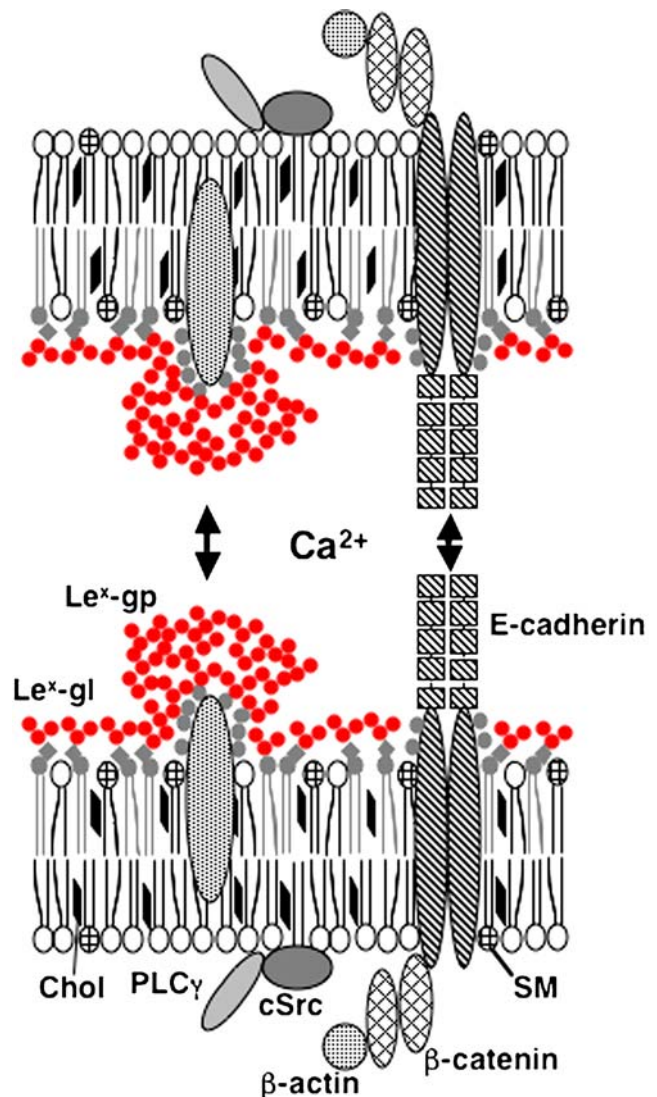


Fig. 8 A hypothetical model for the membrane microdomain-mediated cell–cell interaction during epiboly in medaka gastrula. Membrane microdomain from gastrula embryos is a cholesterol (*Chol*)- and sphingomyelin (*SM*)-enriched membrane. A cell adhesion molecule complex (*E-cadherin*, β -*catenin*), transducer proteins (*PLC γ* , *cSrc*), and a cytoskeleton protein (β -*actin*) are enriched. Le^X -containing glycolipid (Le^X -*gl*) and glycoprotein (Le^X -*gp*) are exclusively concentrated. E-cadherin may form a complex with β -*catenin* and β -*actin* at the cytoplasmic domain. One membrane microdomain binds to E-cadherin on the other through E-cadherin and Le^X -glycans. E-cadherin on one membrane microdomain binds to E-cadherin on the other through its extracellular domain. Le^X -glycans of Le^X -glycolipid and Le^X -gp mediate the membrane microdomain interaction through binding to those Le^X -glycans or a Le^X -binding lectin on the counterpart membrane microdomain. cSrc and PLC γ may be associated with E-cadherin activation and some growth factor receptor (*e.g.*, FGF receptor) signaling. The membrane microdomain is a platform for E-cadherin- and Le^X -glycan-mediated cell adhesion and the subsequent signal transduction

the inhibitory HAD peptide (Fig. 5). Cadherin is a type 1 transmembrane protein that contains five Ig-like extracellular (EC) domains in a rod-like conformation stabilized by interdomain calcium atoms. Particular decapeptide sequences in the EC1 domain are known to inhibit the homophilic binding of cadherin [45]. The HAD peptide for inhibition of the E-cadherin homophilic binding was designed from the amino acid sequence of EC1 domain of medaka E-cadherin⁶. The LD-DIM homotypic binding was inhibited by 30% and 60% in the presence of 1 μ M and 10 μ M HAD, respectively, showing that the inhibition by the HAD peptide was saturated. Therefore, the E-cadherin-mediated binding partially contributes to the LD-DIM homotypic binding. Consistent with these results, the LD-DIM binding to the protease-digested LD-DIM on the solid surface was decreased by 40% of those to the undigested LD-DIM (Fig. 4). These results indicate that contribution of the E-cadherin-mediated binding to the LD-DIM homotypic binding is largely 50%.

Involvement of the Le^X-glycans in the LD-DIM homotypic binding was shown by the following lines of evidence. First, the binding of LD-DIM to the fucosidase-digested LD-DIM on the solid surface was decreased. This fucosidase specifically acts on the α 1 \rightarrow 3- and α 1 \rightarrow 4-linkages of Fuc. The extent of the decrease of binding on the fucosidase digestion was 53%, and a partial involvement of α 1 \rightarrow 3/4Fuc-containing glycan structure is suggested. The presence of Le^X-glycans was clearly demonstrated in the LD-DIM (Figs. 1, 2, and 6). On the other hand, no Le^a-glycan (Gal β 1 \rightarrow 3(Fuc α 1 \rightarrow 4)GlcNAc β 1 \rightarrow) containing α 1 \rightarrow 4-Fuc linkage was detected in the LD-DIM by the immunochemical detection using anti-Le^a antibody (data not shown). We cannot exclude the presence of the α 1 \rightarrow 4-Fuc-containing structures such as sialyl Le^a and Le^b in the LD-DIM, because we could not test their presence due to unavailability of specific antibodies against these structures. Therefore, the LD-DIM binding is mediated at least through Le^X-glycans (Gal β 1 \rightarrow 4(Fuc α 1 \rightarrow 3)GlcNAc β 1 \rightarrow), but not Le^a-glycans. Consistent with this observation, the LD-DIM binding to the periodate-treated LD-DIM on the solid surface was decreased to 50% of that to the untreated LD-DIM (Fig. 4). Previously, the presence of Gal-Le^X-glycan structure (Gal β 1 \rightarrow 4Gal β 1 \rightarrow 4(Fuc α 1 \rightarrow 3)GlcNAc β 1 \rightarrow) in egg cortical vesicular glycoprotein (hyosporin) of medaka was demonstrated [31]. Using monoclonal antibody against Gal-Le^X-glycan, this epitope was shown to present in the LD-DIM at gastrula stages (data not shown). However, whether the Gal-Le^X-glycan also participates in the LD-DIM homotypic binding remains to be elucidated. Second, the

LD-DIM had the ability to bind to Le^X-containing glycans such as neoglycopolypeptides and neoglycolipids. The LD-DIM bound to the PGA containing Le^X-structure (Le^X-PGA), but not to LacNAc-PGA or SiaLe^X-PGA (Fig. 6) The binding to Le^X-PGA did not occur when Le^X-PGA was treated with periodate oxidation. These results suggest that the LD-DIM specifically recognizes the Le^X-structure on the polypeptide. Similarly, the LD-DIM strongly bound to Le^X-Lac-PE, which is a neoglycolipid consisting of PE conjugated with Le^X-Lac oligosaccharide, while far less binding takes place with Le^a-Lac-PE or H-Lac-PE, containing Fuc α 1 \rightarrow 4GlcNAc or Fuc α 1 \rightarrow 2Gal-linkage, respectively. All these results also indicate that the LD-DIM homotypic binding is mediated through Le^X-glycans on the LD-DIM.

Le^X is one of the Lewis blood group antigens and also known as CD15. In addition, Le^X shares the same epitope structure with SSEA-1, one of the stage specific embryonic antigens [52]. The Le^X was first identified as the antigen that is only detected in undifferentiated F9 teratocarcinoma cells, but not in the differentiated cells [53]. Strong expression of Le^X is also transiently observed at 8-cell to compaction stages in mouse embryogenesis [54, 55]. The Le^X glycan structure is multiply expressed on the highly branched poly-lactosaminoglycan chain(s) [56]. Since free Le^X glycans inhibit the cell–cell interaction during compaction [40, 57] and the aggregation of teratocarcinoma [41], Le^X-glycans are shown to play important roles in cell–cell interaction in embryogenesis. Interestingly, the Le^X-glycans are shown to bind to each other [41], and the Le^X–Le^X interaction is considered to contribute to those cell–cell interactions [41]. Le^X-glycans are also expressed on the stem cell of rabbit cornea, and implicate in regulation of cell growth and optical differentiation [58]. The expression of the Le^X-epitope on the cornea decreases as the optical differentiation goes on. A role of Le^X-glycans in the cornea stem cell remains unknown. By analogy with the mouse compaction phenomenon, it is likely that Le^X on the LD-DIM is involved in the cell–cell adhesion in medaka gastrula embryos through the Le^X–Le^X interaction. However, we cannot exclude the possibility that a Le^X-binding C-type lectin is present on the LD-DIM. In mammals, mMGL2 [59], DC-SIGN [60] and the scavenger receptor C-type lectin [61] are shown to be a Le^X-binding lectin.

How the E-cadherin- and Le^X-glycan-mediated interactions are involved in the membrane microdomain-mediated cell–cell interactions on the surface of developing embryos remains unknown. The co-immunoprecipitation experiments using anti-EC1 antibody (Fig. 7) showed that E-cadherin and Le^X-gp are co-localized on the same membrane microdomain, while these two proteins are not strongly associated with each other unlike the case with E-cadherin and β -catenin. E-cadherin does not contain Le^X-structure on its

⁶ Adachi, T., Sato, C., Hashimoto, H., Wakamatsu, Y., and Kitajima, K., to be published elsewhere.

glycan moieties, and Le^X-gp is a major glycoprotein bearing the Le^X-structure. Therefore, the E-cadherin- and Le^X-glycan-mediated interactions can work independently, but are operative at the same time on the same membrane microdomain. As described above, contributions of these two interactions to the homotypic LD-DIM binding are largely even, when the LD-DIM was prepared from early gastrula (12 hpf) embryos. However, the expression of Le^X-gp on the LD-DIM starts at early gastrula and greatly increases until at least 2–4 somite stage (30 hpf; Fig. 3). The contribution of the Le^X-glycan-mediated interaction must change depending on the developmental stages. Therefore, it is important to know how the LD-DIM homotypic binding is regulated by the expression levels of E-cadherin and Le^X-gp, and effects of suppression of gene expression for E-cadherin and/or fucosyltransferases required for the synthesis of Le^X-structure on the process of epiboly are being examined in our laboratory.

In our previous study, we have demonstrated that LD-DIM prepared from sea urchin sperm has the ability to bind to sperm binding protein (SBP) on the egg vitelline layer. The sperm LD-DIM is suggested to function as a platform of sperm binding to SBP on the sperm-egg binding [10, 16, 17]. The binding of the LD-DIM to SBP depends on the disialyl epitope, Neu5Acα2→8Neu5Acα2→, on the LD-DIM. Notably, the disialyl epitope is a common epitope between glycoprotein and glycolipid in the LD-DIM from sea urchin sperm [62], although which disialyl epitope is involved in the LD-DIM-SBP binding remains unknown. In medaka gastrula embryo, Le^X-gp and Le^X-glycolipid are exclusively localized in the LD-DIM, and the Le^X-epitope is a common glycan epitope expressed both on glycoprotein and glycolipid in the LD-DIM. If we consider that the Le^X-epitope on the membrane microdomains is involved in cell adhesion during the progress of epiboly, it would be interesting to demonstrate that a common glycan structure shared by glycoproteins and glycolipids on the LD-DIM might be functional in a LD-DIM-mediated binding in other biological processes.

Acknowledgments *This work was supported in part by Grants-in-Aids for CREST of Japan Science and Technology Corporation (to KK), and for Young Scientists (B) (18770083) from the Ministry of Education, Science, Sports and Culture. We thank Professor Tsukasa Matsuda (Nagoya University) for his valuable discussion and constant encouragement all through this work.

References

1. Simons, K., Ikonen, E.: Functional rafts in cell membranes. *Nature* **387**, 569–572 (1997). doi:10.1038/42408
2. Brown, D.A., Rose, J.K.: Sorting of GPI-anchored proteins to glycolipid-enriched membrane subdomains during transport to the apical cell surface. *Cell* **68**, 533–544 (1992). doi:10.1016/0092-8674(92)90189-J
3. Verkade, P., Simons, K.: Lipid microdomains and membrane trafficking in mammalian cells. *Histochem. Cell Biol.* **108**, 211–220 (1997). doi:10.1007/s004180050161
4. Brown, D.A., London, E.: Structure of detergent-resistant membrane domains: does phase separation occur in biological membranes? *Biochem. Biophys. Res. Commun.* **240**, 1–7 (1997). doi:10.1006/bbrc.1997.7575
5. Kenworthy, A.K., Edidin, M.: Distribution of a glycosylphosphatidylinositol-anchored protein at the apical surface of MDCK cells examined at a resolution of <100 Å using imaging fluorescence resonance energy transfer. *J. Cell Biol.* **142**, 69–84 (1998). doi:10.1083/jcb.142.1.69
6. Yamamura, S., Handa, K., Hakomori, S.: A close association of GM3 with c-Src and Rho in GM3-enriched microdomains at the B16 melanoma cell surface membrane: a preliminary note. *Biochem. Biophys. Res. Commun.* **236**, 218–222 (1997). doi:10.1006/bbrc.1997.6933
7. Kasahara, K., Watanabe, Y., Yamamoto, T., Sanai, Y.: Association of Src family tyrosine kinase Lyn with ganglioside GD3 in rat brain. Possible regulation of Lyn by glycosphingolipid in caveolae-like domains. *J. Biol. Chem.* **272**, 29947–29953 (1997). doi:10.1074/jbc.272.47.29947
8. Maekawa, S., Sato, C., Kitajima, K., Funatsu, N., Kumanogoh, H., Sokawa, Y.: Cholesterol-dependent localization of NAP-22 on a neuronal membrane microdomain (raft). *J. Biol. Chem.* **274**, 21369–21374 (1999). doi:10.1074/jbc.274.30.21369
9. Mañes, S., Mira, E., Gómez-Moutón, C., Lacalle, R.A., Keller, P., Labrador, J.P., *et al.*: Membrane raft microdomains mediate front-rear polarity in migrating cells. *EMBO J.* **18**, 6211–6220 (1999). doi:10.1093/emboj/18.22.6211
10. Ohta, K., Sato, C., Matsuda, T., Toriyama, M., Lennarz, W.J., Kitajima, K.: Isolation and characterization of low density detergent-insoluble membrane (LD-DIM) fraction from sea urchin sperm. *Biochem. Biophys. Res. Commun.* **258**, 616–623 (1999). doi:10.1006/bbrc.1999.0686
11. Harder, T., Simons, K.: Caveolae, DIGs, and the dynamics of sphingolipid-cholesterol microdomains. *Curr. Opin. Cell Biol.* **9**, 534–542 (1997). doi:10.1016/S0955-0674(97)80030-0
12. Song, Y., Withers, D.A., Hakomori, S.: Globoside-dependent adhesion of human embryonal carcinoma cells, based on carbohydrate-carbohydrate interaction, initiates signal transduction and induces enhanced activity of transcription factors AP1 and CREB. *J. Biol. Chem.* **273**, 2517–2525 (1998). doi:10.1074/jbc.273.5.2517
13. Iwabuchi, K., Handa, K., Hakomori, S.: Separation of “glycosphingolipid signaling domain” from caveolin-containing membrane fraction in mouse melanoma B16 cells and its role in cell adhesion coupled with signaling. *J. Biol. Chem.* **273**, 33766–33773 (1998). doi:10.1074/jbc.273.50.33766
14. Iwabuchi, K., Yamamura, S., Prinetti, A., Handa, K., Hakomori, S.: GM3-enriched microdomain involved in cell adhesion and signal transduction through carbohydrate-carbohydrate interaction in mouse melanoma B16 cells. *J. Biol. Chem.* **273**, 9130–9138 (1998). doi:10.1074/jbc.273.15.9130
15. Prinetti, A., Iwabuchi, K., Hakomori, S.: Glycosphingolipid-enriched signaling domain in mouse neuroblastoma Neuro2a cells. Mechanism of ganglioside-dependent neuritogenesis. *J. Biol. Chem.* **274**, 20916–20924 (1999). doi:10.1074/jbc.274.30.20916
16. Ohta, K., Sato, C., Matsuda, T., Toriyama, M., Vacquier, V.D., Lennarz, W.J., *et al.*: Co-localization of receptor and transducer proteins in the glycosphingolipid-enriched, low density, detergent-insoluble membrane fraction of sea urchin sperm. *Glycoconj. J.* **17**, 205–214 (2000). doi:10.1023/A:1026589223811

17. Maehashi, E., Sato, C., Ohta, K., Harada, Y., Matsuda, T., Hirohashi, N., *et al.*: Identification of the sea urchin 350-kDa sperm-binding protein as a new sialic acid-binding lectin that belongs to the heat shock protein 110 family: implication of its binding to gangliosides in sperm lipid rafts in fertilization. *J. Biol. Chem.* **278**, 42050–42057 (2003). doi:10.1074/jbc.M307493200
18. Adachi, T., Sato, C., Kitajima, K.: Membrane microdomain formation is crucial in epiboly during gastrulation of medaka. *Biochem. Biophys. Res. Commun.* **358**, 848–853 (2007). doi:10.1016/j.bbrc.2007.04.197
19. Ilangumaran, S., Hoessli, D.C.: Effects of cholesterol depletion by cyclodextrin on the sphingolipid microdomains of the plasma membrane. *Biochem. J.* **335**, 433–440 (1998)
20. Simon, C.G., Gear, A.R.: Membrane-destabilizing properties of C2-ceramide may be responsible for its ability to inhibit platelet aggregation. *Biochemistry* **37**, 2059–2069 (1998). doi:10.1021/bi9710636
21. Iwamatsu, T.: Stages of normal development in the medaka *Oryzias latipes*. *Mech. Dev.* **121**, 605–618 (2004). doi:10.1016/j.mod.2004.03.012
22. Stoll, M.S., Mizuochi, T., Childs, R.A., Feizi, T.: Improved procedure for the construction of neoglycolipids having antigenic and lectin-binding activities, from reducing oligosaccharides. *Biochem. J.* **256**, 661–664 (1988)
23. Feizi, T., Stoll, M.S., Yuen, C.T., Chai, W., Lawson, A.M.: Neoglycolipids: probes of oligosaccharide structure, antigenicity, and function. *Methods Enzymol.* **230**, 484–519 (1994). doi:10.1016/0076-6879(94)30030-5
24. Kobayashi, K., Tawada, E., Akaike, T., Usui, T.: Artificial glycopeptide conjugates: simple synthesis of lactose- and *N,N*-diacetylchitobiose-substituted poly(L-glutamic acid)s through *N*-beta-glycoside linkages and their interaction with lectins. *Biochim. Biophys. Acta* **1336**, 117–122 (1997)
25. Totani, K., Kubota, T., Kuroda, T., Murata, T., Hidari, K.I., Suzuki, T., *et al.*: Chemoenzymatic synthesis and application of glycopolymers containing multivalent sialyloligosaccharides with a poly(L-glutamic acid) backbone for inhibition of infection by influenza viruses. *Glycobiology* **13**, 315–326 (2003). doi:10.1093/glycob/cwg032
26. Mañes, S., Mira, E., Gómez-Moutón, C., Lacalle, R.A., Keller, P., Labrador, J.P., *et al.*: Membrane raft microdomains mediate front-rear polarity in migrating cells. *EMBO J.* **18**, 6211–6220 (1999). doi:10.1093/emboj/18.22.6211
27. Sato, C., Kitajima, K., Inoue, S., Seki, T., Troy 2nd, F.A., Inoue, Y.: Characterization of the antigenic specificity of four different anti-(alpha 2->8-linked polysialic acid) antibodies using lipid-conjugated oligo/polysialic acids. *J. Biol. Chem.* **270**, 18923–18928 (1995). doi:10.1074/jbc.270.32.18923
28. Higashi, H., Fukui, Y., Ueda, S., Kato, S., Hirabayashi, Y., Matsumoto, M., *et al.*: Sensitive enzyme-immunostaining and densitometric determination on thin-layer chromatography of N-glycolylneuraminic acid-containing glycosphingolipids, Hanganutziu-Deicher antigens. *J. Biochem.* **95**, 1517–1520 (1984)
29. Song, Y., Kitajima, K., Inoue, Y.: Monoclonal antibody specific to alpha-2->3-linked deaminated neuraminyl beta-galactosyl sequence. *Glycobiology* **3**, 31–36 (1993). doi:10.1093/glycob/3.1.31
30. Sato, C., Fukuoka, H., Ohta, K., Matsuda, T., Koshino, R., Kobayashi, K., *et al.*: Frequent occurrence of pre-existing alpha 2->8-linked disialic and oligosialic acids with chain lengths up to 7 Sia residues in mammalian brain glycoproteins. Prevalence revealed by highly sensitive chemical methods and anti-di-, oligo-, and poly-Sia antibodies specific for defined chain lengths. *J. Biol. Chem.* **275**, 15422–15431 (2000). doi:10.1074/jbc.275.20.15422
31. Taguchi, T., Seko, A., Kitajima, K., Muto, Y., Inoue, S., Khoo, K. H., *et al.*: Structural studies of a novel type of pentaantennary large glycan unit in the fertilization-associated carbohydrate-rich glycopeptide isolated from the fertilized egg of *Oryzias latipes*. *J. Biol. Chem.* **269**, 8762–8771 (1994)
32. Harder, T., Scheiffle, P., Verkade, P., Simons, K.: Lipid domain structure of the plasma membrane revealed by patching of membrane components. *J. Cell Biol.* **141**, 929–942 (1998). doi:10.1083/jcb.141.4.929
33. Villalba, M., Bi, K., Hu, J., Altman, Y., Bushway, P., Reits, E., *et al.*: Translocation of PKC[theta] in T cells is mediated by a nonconventional, PI3-K- and Vav-dependent pathway, but does not absolutely require phospholipase C. *J. Cell Biol.* **157**, 253–263 (2002). doi:10.1083/jcb.200201097
34. Hur, E.M., Park, Y.S., Lee, B.D., Jang, I.H., Kim, H.S., Kim, T. D., *et al.*: Sensitization of epidermal growth factor-induced signaling by bradykinin is mediated by c-Src. Implications for a role of lipid microdomains. *J. Biol. Chem.* **279**, 5852–5860 (2004). doi:10.1074/jbc.M311687200
35. Ryan, P.J., Gillespie, L.L.: Phosphorylation of phospholipase C gamma 1 and its association with the FGF receptor is developmentally regulated and occurs during mesoderm induction in *Xenopus laevis*. *Dev. Biol.* **166**, 101–111 (1994). doi:10.1006/dbio.1994.1299
36. Weinstein, D.C., Hemmati-Brivanlou, A.A.: Src family kinase function during early *Xenopus* development. *Dev. Dyn.* **220**, 163–168 (2001). doi:10.1002/1097-0177(2000)9999:9999<1::AID-DVDY1098>3.0.CO;2-5
37. Ozawa, M., Baribault, H., Kemler, R.: The cytoplasmic domain of the cell adhesion molecule uvomorulin associates with three independent proteins structurally related in different species. *EMBO J.* **8**, 1711–1717 (1989)
38. Hope, H.R., Pike, L.J.: Phosphoinositides and phosphoinositide-utilizing enzymes in detergent-insoluble lipid domains. *Mol. Biol. Cell* **7**, 843–851 (1996)
39. Arvanitis, D.N., Min, W., Gong, Y., Heng, Y.M., Boggs, J.M.: Two types of detergent-insoluble, glycosphingolipid/cholesterol-rich membrane domains from isolated myelin. *J. Neurochem.* **94**, 1696–1710 (2005). doi:10.1111/j.1471-4159.2005.03331.x
40. Fenderson, B.A., Zehavi, U., Hakomori, S.: A multivalent lacto-*N*-fucose pentaaose III-lysyllysine conjugate decompacts preimplantation mouse embryos, while the free oligosaccharide is ineffective. *J. Exp. Med.* **160**, 1591–1596 (1984). doi:10.1084/jem.160.5.1591
41. Eggens, I., Fenderson, B., Toyokuni, T., Dean, B., Stroud, M., Hakomori, S.: Specific interaction between Lex and Lex determinants. A possible basis for cell recognition in preimplantation embryos and in embryonal carcinoma cells. *J. Biol. Chem.* **264**, 9476–9484 (1989)
42. Kemler, R., Babinet, C., Eisen, H., Jacob, F.: Surface antigen in early differentiation. *Proc. Natl. Acad. Sci. USA* **74**, 4449–4452 (1977). doi:10.1073/pnas.74.10.4449
43. Hyafil, F., Morello, D., Babinet, C., Jacob, F.: A cell surface glycoprotein involved in the compaction of embryonal carcinoma cells and cleavage stage embryos. *Cell* **21**, 927–934 (1980). doi:10.1016/0092-8674(80)90456-0
44. Haseley, S.R., Vermeer, H.J., Kammerling, J.P., Vliegthart, J.F.: Carbohydrate self-recognition mediates marine sponge cellular adhesion. *Proc. Natl. Acad. Sci. USA* **98**, 9419–9424 (2001). doi:10.1073/pnas.151111298
45. Noë, V., Willems, J., Vandekerckhove, J., Roy, F.V., Bruyneel, E., Mareel, M.: Inhibition of adhesion and induction of epithelial cell invasion by HAV-containing E-cadherin-specific peptides. *J. Cell Sci.* **112**, 127–135 (1999)
46. Yoshida, C., Takeichi, M.: Teratocarcinoma cell adhesion: identification of a cell-surface protein involved in calcium-dependent cell aggregation. *Cell* **28**, 217–224 (1982). doi:10.1016/0092-8674(82)90339-7
47. Nagafuchi, A., Takeichi, M.: Transmembrane control of cadherin-mediated cell adhesion: a 94 kDa protein functionally associated

- with a specific region of the cytoplasmic domain of E-cadherin. *Cell Regul.* **1**, 37–44 (1989)
48. Ozawa, M., Ringwald, M., Kemler, R.: Uvomorulin-catenin complex formation is regulated by a specific domain in the cytoplasmic region of the cell adhesion molecule. *Proc. Natl. Acad. Sci. USA* **87**, 4246–4250 (1990). doi:10.1073/pnas.87.11.4246
49. Solnica-Krezel, L.: Conserved patterns of cell movements during vertebrate gastrulation. *Curr. Biol.* **15**, R213–R228 (2005). doi:10.1016/j.cub.2005.03.016
50. Tsukita, S., Oishi, K., Akiyama, T., Yamanashi, Y., Yamamoto, T.: Specific proto-oncogenic tyrosine kinases of src family are enriched in cell-to-cell adherens junctions where the level of tyrosine phosphorylation is elevated. *J. Cell Biol.* **113**, 867–879 (1991). doi:10.1083/jcb.113.4.867
51. McLachlan, R.W., Kraemer, A., Helwani, F.M., Kovacs, E.M., Yap, A.S.: E-cadherin adhesion activates c-Src signaling at cell–cell contacts. *Mol. Biol. Cell* **18**, 3214–3223 (2007). doi:10.1091/mbc.E06-12-1154
52. Solter, D., Knowles, B.B.: Monoclonal antibody defining a stage-specific mouse embryonic antigen (SSEA-1). *Proc. Natl. Acad. Sci. USA* **75**, 5565–5569 (1978). doi:10.1073/pnas.75.11.5565
53. Solter, D., Knowles, B.B.: Developmental stage-specific antigens during mouse embryogenesis. *Curr. Top. Dev. Biol.* **13**, 139–165 (1979). doi:10.1016/S0070-2153(08)60693-6
54. Fenderson, B.A., Eddy, E.M., Hakomori, S.: Glycoconjugate expression during embryogenesis and its biological significance. *Bioessays* **12**, 173–179 (1990). doi:10.1002/bies.950120406
55. Gomperts, M., Garcia-Castro, M., Wylie, C., Heasman, J.: Interactions between primordial germ cells play a role in their migration in mouse embryos. *Development* **120**, 135–141 (1994)
56. Ozawa, M., Muramatsu, T.: The glycoprotein-bound large carbohydrates from embryonal carcinoma cells carry receptors for several lectins recognizing *N*-acetylgalactosamine and galactose. *J. Biochem.* **97**, 317–324 (1995)
57. Bird, J.M., Kimber, S.J.: Oligosaccharides containing fucose linked alpha(1–3) and alpha(1–4) to *N*-acetylglucosamine cause decompaction of mouse morulae. *Dev. Biol.* **104**, 449–460 (1984). doi:10.1016/0012-1606(84)90101-5
58. Cao, Z., Zhao, Z., Mohan, R., Alroy, J., Stanley, P., Panjwani, N.: Role of the Lewis(x) glycan determinant in corneal epithelial cell adhesion and differentiation. *J. Biol. Chem.* **276**, 21714–21723 (2001)
59. Tsuiji, M., Fujimori, M., Ohashi, Y., Higashi, N., Onami, T.M., Hedrick, S.M., *et al.*: Molecular cloning and characterization of a novel mouse macrophage C-type lectin, mMGL2, which has a distinct carbohydrate specificity from mMGL1. *J. Biol. Chem.* **277**, 28892–28901 (2002). doi:10.1074/jbc.M203774200
60. van Die, I., van Vliet, S.J., Nyame, A.K., Cummings, R.D., Bank, C.M., Appelmek, B., *et al.*: The dendritic cell-specific C-type lectin DC-SIGN is a receptor for *Schistosoma mansoni* egg antigens and recognizes the glycan antigen Lewis x. *Glycobiology* **13**, 471–478 (2003). doi:10.1093/glycob/cwg052
61. Coombs, P.J., Graham, S.A., Drickamer, K., Taylor, M.E.: Selective binding of the scavenger receptor C-type lectin to Lewisx trisaccharide and related glycan ligands. *J. Biol. Chem.* **280**, 22993–22999 (2005). doi:10.1074/jbc.M504197200
62. Miyata, S., Sato, C., Kitamura, S., Toriyama, M., Kitajima, K.: A major flagellum sialoglycoprotein in sea urchin sperm contains a novel polysialic acid, an alpha2,9-linked poly-*N*-acetylneuraminic acid chain, capped by an 8-*O*-sulfated sialic acid residue. *Glycobiology* **14**, 827–840 (2004). doi:10.1093/glycob/cwh100